Int J Fract (2020) 226:71–79
https://doi.org/10.1007/s10704-020-00479-7

ORIGINAL PAPER

Energy release rate of a single edge cracked specimen subjected to large deformation

Zezhou Liu · Michael Zakoworotny · Jingyi Guo · Alan T. Zehnder · Chung-Yuen Hui

Received: 8 June 2020 / Accepted: 20 August 2020 / Published online: 7 September 2020

Abstract The single edge notch specimen (SEN) is commonly used to measure the fracture toughness, or critical energy release rate of soft elastic materials. To measure toughness, an expression for the energy release rate, J, the mechanical energy available for growing the crack per unit area, is needed. Since strains in these fracture experiments can easily exceed several hundred percent, large deformation analysis is needed to calculate J. An approximate formula for J in SEN samples subjected to moderately large deformation was given by Rivlin and Thomas in J Polym Sci 10:291–318. https://doi.org/10.1002/pol.1953.120100303 (1953) and Greensmith in J Appl Polymer Sci 7:993–1002. https://doi.org/10.1002/app.1963.070070316 (1963). However, this formula works only for small crack lengths, for stretch ratio up to two and does not match the linear elastic result in the limit of small strains. In this paper we carry out a series of finite element (FE) simulations to obtain accurate approximations that are valid for all practical crack lengths and strain levels. Our FE result shows that the small crack approximation of by Rivlin and Thomas in J Polym Sci 10:291–318. https://doi.org/10.1002/pol.1953.120100303 (1953) does not work well in the small strain regime, and in particular, result of Greensmith in J Appl Polymer Sci 7:993–1002. https://doi.org/10.1002/app.1963.070070316 (1963) underestimates the energy release rate for stretch ratios less than 1.5.

Keywords Single edge notch specimen · Energy release rate · Large deformation · Finite element method

Electronic supplementary material The online version of this article (https://doi.org/10.1007/s10704-020-00479-7) contains supplementary material, which is available to authorized users.

Z. Liu · J. Guo · A. T. Zehnder · C.-Y. Hui (✉)
Field of Theoretical and Applied Mechanics, Sibley School of Mechanical and Aerospace Engineering, Cornell University, Ithaca, NY 14853, USA
e-mail: ch45@cornell.edu

M. Zakoworotny
Sibley School of Mechanical and Aerospace Engineering, Cornell University, Ithaca, NY 14853, USA

C.-Y. Hui
Global Station for Soft Matter, GI-CoRE, Hokkaido University, Sapporo, Japan

1 Introduction and previous works

Recent advances in soft materials, especially the ability to make highly compliant and tough hydrogels (Gong et al. 2003; Sun et al. 2012) have renewed interest in the study of fracture behavior of elastic, stretchable materials (Tanaka et al. 2005; Kundu and Crosby 2009; Sun et al. 2012; Kim et al. 2020). In elastic solids, the driving force for crack growth is the energy release rate J, defined as the change in the sum of the elastic strain energy stored in the crack specimen and the potential energy of the loading system per unit area of crack growth. The resistance to fracture is usually character-

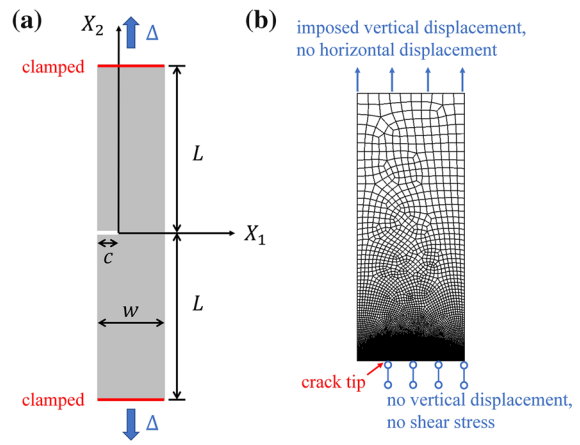

Fig. 1 **a** Undeformed stress free (reference) configuration of a SEN specimen. The specimen has thickness t in the out of plane direction. Plane stress condition requires $L, w >> t$ and $c >> t$. **b** Finite element model using symmetry boundary conditions along $X_2 = 0$

ized by the fracture toughness G_c which is defined as the *critical energy release rate* for a pre-existing crack to grow. While the fracture toughness is a material property, the energy release rate J depends on the manner of loading as well as the specimen geometry. In testing, one chooses a specimen with a pre-existing crack, computes the energy release rate J as a function of load and geometry, and determines G_c by noting that crack growth occurs when J reaches G_c.

The single edge notched (SEN) specimen is shown schematically in Fig. 1a. The undeformed sample is a long strip of length $2L$, width w and thickness t with $t << w < 2L$. A crack of initial length c is cut from the edge of the specimen. Greensmith (1963) employed this specimen to determine the fracture toughness of four vulcanized rubbers. It is a popular specimen to study the fracture behavior of hydrogels since the same specimen without a crack can be used to measure tensile properties (Greensmith 1963; Lindley 1972; Hamed and Park 1999; Yeoh 2002; Lin et al. 2010, 2011; Kwon et al. 2011; Ducrot et al. 2014; Mayumi et al. 2016; Chen et al. 2017; Morelle et al. 2018; Roucou et al. 2018; Bai et al. 2018).

Although accurate expressions of J for SEN can be found in Tada et al. (2000), these expressions are based on linear elastic fracture mechanics (LEFM) and can lead to large errors when applied to soft samples subjected to large deformation (see the Electronic Supplementary Material (ESM) for more detailed discussions). The only available expression for J which accounts for large deformation is given by Rivlin and Thomas (1953). They used dimensional analysis to show that for *small* cracks of length c, i.e $c/w << 1$, J is

$$J = 2K(\lambda) W_0(\lambda) c, \tag{1}$$

where $\lambda \equiv 1 + (\Delta/L)$ is the applied stretch ratio (Δ is the displacement at the grips, i.e., at $X_2 = \pm L$ in Fig. 1a), $W_0(\lambda)$ is the elastic strain energy density of an *uncracked* sample ($c = 0$) subjected to the same stretch ratio λ and $K(\lambda)$ is a numerical factor that varies only with λ. In Rivlin and Thomas (1953), the material is assumed to be incompressible and isotropic, so W_0 depends only on the strain invariants $I_1 = \mathrm{tr}\mathbf{C}$ and $I_2 = \left[(\mathrm{tr}\mathbf{C})^2 - \mathrm{tr}\mathbf{C}^2\right]/2$, where $\mathbf{C}$ is the right Cauchy Green tensor. The numerical factor $K(\lambda)$ in (1) was determined empirically by Greensmith (1963) by conducting experiments on four Gum vulcanized natural rubbers. The stretch ratios in these experiments range from 1.05 to 2 (corresponding to nominal strains of 5 to 100 percent). Within this range of λ, Greensmith (1963) reported that the stress versus stretch behavior of all four rubbers in simple extension obeys the Mooney-Rivlin (MR) model. It should be noted that the applied extension ratio λ in fracture testing of hydrogels can be much larger. For example, in some very tough hydrogels, λ can exceed 10 (Sun et al. 2012).

The factor $K(\lambda)$ was given graphically in Fig. 5 of Greensmith's work. Cristiano et al. (2011) suggested the following approximation for $K(\lambda)$

$$K(\lambda) = \frac{3}{\sqrt{\lambda}}, \quad 1 < \lambda \leq 2 \tag{2a}$$

A similar expression for $K(\lambda)$ was proposed earlier by Lindley (1972) where

$$K(\lambda) = \frac{2.95 - 0.08(1-\lambda)}{\sqrt{\lambda}}, \quad 1 < \lambda \leq 2 \tag{2b}$$

There are limitations in (1) and (2a,b). First, it requires small crack lengths, $c/w << 1$. Rivlin and Thomas (1953) suggested $c/w < 0.2$; however, (2a,b) is often used to determine energy release rate for longer cracks (Cristiano et al. 2011; Kwon et al. 2011). Second, the data and calculations which support its validity are limited to stretch ratios between 1.05 to 2 whereas tough hydrogel crack specimens fail at considerably higher extensions (Sun et al. 2012). Third, since not all material behavior can be fit by the MR model, it is commonly assumed that K is *independent* of the strain

energy density function. However, there is no theoretical basis for this assumption even for small cracks. Indeed, Yeoh (2002) has carried out numerical studies for *small* cracks in a MR and a three term Yeoh's (cubic) solid. For strains greater than 20%, he found substantial difference in K for the cubic and MR solids. Finally, a minor point, both (2a) and (2b) underestimate K as $\lambda \to 1$. Greensmith's data, when extrapolate to $\lambda = 1$, is close to π. Yeoh (2002) and Lindley (1972) observed that the energy release rates given by (2a) and (2b) *do not approach* the *small strain* energy release rate J for small cracks, which is

$$J\left(c/w_0 << 1, \lambda \approx 1\right) = 2\pi\left[1.1215\right]^2 W_0\left(\varepsilon\right) c \Rightarrow K\left(\lambda \to 1\right) = \pi\left[1.1215\right]^2 \approx 3.95, \quad (3)$$

where $W_0\left(\varepsilon\right) = E\varepsilon^2/2$ with E the Young's modulus and ε the strain. The behavior of (2a) for small strains is

$$J_s = 6W_0\left(\varepsilon\right) c \Rightarrow K\left(\lambda \to 1\right) = 3. \quad (4)$$

The theoretical limit given by (3) is about 24% *higher* than the $K\left(\lambda \to 1\right)$ given by (4), and still 21% higher even if we take $K\left(\lambda \to 1\right) = \pi$ which is extrapolated using Greensmith's data. Greensmith (1963) was aware of this discrepancy. Based on the solution of the *center* crack in an infinite plate, he suggested in the discussion that $K\left(\lambda \to 1\right)$ should be close to but not exactly π. He overlooked, however, that the solution of the edge crack in an infinite plate problem was solved earlier by Wigglesworth where $K\left(\lambda \to 1\right)$ is, within one unit of last digit, given by $\left(1.1215\right)^2\pi \approx 1.26\pi$ (Wigglesworth 1957). Lindley (1972) and Yeoh (2002) have carried out *plane stress* finite element calculations to determine $K\left(\lambda\right)$ for short cracks and for $1 < \lambda \leq 2.5$. Their numerical results show reasonable agreement with Greensmith's data. However, their FE results for short cracks and small strains cannot be correct since they do not converge to the theoretical limit given by (3). In contrast, our numerical result in the next section (and the ESM) approaches this theoretical limit. Details of comparison with the numerical results of Lindley are given in the ESM.

Our analysis above still does not explain why Greensmith's *experimental* data differs from the theoretical limit given by (3). We offer three possibilities. The first being that it is difficult to conduct experiments in the regime of small cracks and small strains. For example, Lindley (1972) also conducted experiments on small crack samples. His $K\left(\lambda\right)$ for $\lambda = 1.25$ is 2.66 whereas Greensmith's value is slightly below 2.5. This discrepancy suggests there can be considerable experimental errors in this regime. A different source of error which has been ignored by many investigators is the 3D effects. The implicit assumption in all the analysis (theoretical and numerical) is to assume that plane stress condition prevails. However, this cannot be the case when *c is on the order of the plate thickness t*. Specifically, plane stress requires $c >> t$. Thus, when $c \approx t$, the 3D effects can become significant. Indeed, when the crack is sufficiently small so that $c << t$, plane strain condition must prevail. This means that the *plane stress* energy release rate J given by (3) must be replaced by the *plane strain* energy release rate. This leads to a reduction of J by a factor of 3/4 due to incompressibility, i.e.,

$$J^{pl-strain}\left(c/t << 1, \lambda \to 1\right) = \frac{3}{4} \times 2\pi\left[1.1215\right]^2 W_0\left(\varepsilon\right) c \approx 5.93 W_0\left(\varepsilon\right) c. \quad (5)$$

Note, for very small cracks, (5) is consistent with (2a) and (2b) in the limit of small strains. This argument is also consistent with 3D finite element calculations. For example, Kwon and Sun (2000) have carried out detailed 3D FE analysis on a linear elastic plate with a *center* crack with different c/t values, where c is the length of the center crack in their notation. Their FE result shows that when $c \geq 8t$, there is no difference between the through thickness average of the 3D energy release rate and the *plane stress* energy release rate. The 3D energy release rate decreases and approaches the *plane strain* energy release rate when $c/t \leq 1/4$. It should be noted that their calculations are based on a Poisson's ratio of 0.3. The difference in energy release rates would be larger for incompressible solids. The first eight cracked samples in Fig. 3 of Greensmith have lengths *less* than $8t$: the smallest of these cracks has length 0.224cm giving $c/t = 2.24$. This suggests that the 3D effects are present in these samples. However, it must be noted that all these crack lengths are greater than 2mm whereas the plate thickness is 1 mm so the plane strain condition $c/t \leq 1/4$ has not been reached. Hence the 3D effects cannot fully explain why Greensmith's data does not converge to the theoretical limit. Additionally, the data reported in Fig. 3 of Greensmith is for $\lambda = 1.25$ which is probably outside the range of small strain theory. The third possibility is that the small crack approximation proposed by Rivlin and Thomas, (1), is not a good approximation for *small*

strains where $\lambda \approx 1$. To see this, we compare (1) to the LEFM solution which is accurate to within 0.5% for all crack lengths (Tada et al. 2000) (see the ESM for details). Figure S2 in the ESM shows the energy release rate predicted by (1) or (2a, b) has a 50% relative error at $c/w = 0.2$. Even at $c/w = 0.1$, the relative error is about 16%. We consider this last explanation to be the most plausible.

Previous works focused on short cracks and stretch ratios up to 2. *The goal of this work is to provide an accurate expression for the energy release rate that is valid for a much wider range of crack lengths and stretch ratios.* For longer cracks, there is no theoretical basis for (1), hence we explore whether it is possible to write the energy release rate in a *separable* form:

$$J = [2W_0(\lambda, \boldsymbol{\alpha})\, c]\, K(\lambda, \boldsymbol{\alpha})\, f(c/w, w/L) \tag{6}$$

where $W_0(\lambda, \boldsymbol{\alpha})$ is the strain energy density in an uncracked sample in simple extension, $\boldsymbol{\alpha}$ are dimensionless parameters controlling the properties of the strain energy density function, and $K(\lambda, \boldsymbol{\alpha})$ is a loading factor that is independent of geometry. f is a geometrical factor that is independent of applied load. For short cracks (i.e., $c << w$), $f \approx 1$. Specimens are assumed to be sufficiently thin ($c >> t$) so plane stress condition applies. Since most experiments are displacement controlled (to ensure stable crack growth), we impose a uniform stretch ratio λ on the edges $X_2 = \pm L$. We also assume that specimen is perfectly clamped so the lateral displacement on the clamped edge is exactly zero. Since in most experiments $2L$ is about 4 to 6 times of w, all calculations are carried out with $L/w = 2.5$. The crack lengths c in our numerical simulations are between 0.05 and 0.9.

In this work, we consider only incompressible solids. We focus on strain energy densities which depends only on the strain invariant $I_1 = \mathrm{tr}\mathbf{C}$ where $\mathbf{C}$ is the right Cauchy-Green tensor. Even with this simplification, the number of constitutive models for nonlinear elasticity is far too many to explore. Here we consider two models that represent the extreme ends of the spectrum.

$$W^{NH}(I_1) = \frac{\mu}{2}(I_1 - 3) \text{ (neo-Hookean, NH)} \tag{7a}$$

$$W^{AB}(I_1, \boldsymbol{\alpha}) = \mu\sqrt{n}\left[\beta\sqrt{I_1/3} - \sqrt{n}\ln\left(\frac{\sinh\beta}{\beta}\right)\right],$$

$$\beta = \mathcal{L}^{-1}\left(\sqrt{\frac{I_1}{3n}}\right) \text{ (Arruda-Boyce, AB)} \tag{7b}$$

where μ is the small strain shear modulus, n is the number of chain segments and $\mathcal{L}^{-1}$ is the inverse Langevin function. The neo-Hookean model represents the behavior of an ideal rubber whose elasticity is governed purely by chain entropy. This model ignores the finite extensibility of chains and underestimates the stresses at high extension. A model that captures finite extensibility is the Arruda-Boyce's model (7b) (Arruda and Boyce 1993). The factor n in (7b) represents the limit of chain extensibility where the strain energy goes to infinity. In our FEM, we use an alternative form of (7b), which uses the first five terms of the inverse Langevin function, i.e.,

$$W^{AB}(I_1, \boldsymbol{\alpha}) \approx \mu\left[\frac{I_1-3}{2} + \frac{I_1^2-9}{20\lambda_m^2} + \frac{11(I_1^3-27)}{1050\lambda_m^4} + \frac{19(I_1^4-81)}{7000\lambda_m^6} + \frac{519(I_1^5-243)}{673750\lambda_m^8}\right] \tag{8}$$

where $\lambda_m \equiv \sqrt{n}$ is the critical stretch at which the root mean square stretch of the polymer chain, $\sqrt{I_1/3}$, reaches its extensibility limit (Boyce and Arruda 2000). Further, to make contact with Greensmith's work, we also carry out calculations based on the MR model where W is

$$W^{MR} = C_1(I_1 - 3) + C_2(I_2 - 3) \tag{9}$$

The small strain shear modulus is $\mu = 2C_1 + 2C_2$. Mathematically, the neo-Hookean model (NH) (7a) can be considered as a special case of MR model with $C_2 = 0$.

2 Dimensional analysis and separability of J

Dimensional analysis states that

$$J = [2W_0(\lambda, \boldsymbol{\alpha})\, c]\, \bar{J}(\lambda, c/w, w/L, \boldsymbol{\alpha}), \tag{10}$$

where $W_0(\lambda, \boldsymbol{\alpha}) \equiv W(I_1(\lambda), I_2(\lambda), \boldsymbol{\alpha})$ is the energy density in an uncracked sample in simple extension. For example, for the MR solid,

$$W_0(\lambda, \boldsymbol{\alpha}) = C_1\left(\lambda^2 + 2\lambda^{-1} - 3\right) + C_2\left(\lambda^{-2} + 2\lambda - 3\right) \tag{11}$$

Note the normalized energy release rate $\bar{J} = J/[2W_0(\lambda, \boldsymbol{\alpha})\, c]$ in general depends on the choice of *strain energy density function*, the applied stretch ratio λ and the specimen geometry. In particular, except for very small cracks, *the dependence of $\bar{J}$ on the stretch ratio λ may not be factorable to a function K that depends only on λ and a function that depends only on*

geometry. Further, even if this were the case K could still be dependent on the material model. In the following we explore this dependence using three different material models (NH, MR and AB models) with different strain hardening behaviors. Since all our simulations are conducted with $w/L = 2.5$, the dependence of $\bar{J}$on this parameter will not be explicitly indicated in the following section to simplify notations.

The key questions are:

(i) What is the region of validity of (1) or (2a,b)?
(ii) Is J *separable* for a wide range of crack lengths and stretch ratios? Specifically, is it possible to split $\bar{J}$ in (10) into two factors: $\bar{J}(\lambda, c/w, \boldsymbol{\alpha}) = K(\lambda, \boldsymbol{\alpha})\, f(c/w)$ such that $K(\lambda, \boldsymbol{\alpha})$ is *independent of geometry* and $f(c/w)$ is *independent of stretch and material properties*?
(iii) How sensitive is $K(\lambda, \boldsymbol{\alpha})$ to the material model?

A simple observation allows us to address the last two questions using our numerical results. First, $\bar{J} = K(\lambda, \boldsymbol{\alpha})\, f(c/w)$ if and only if $\ln \bar{J} = \ln K(\lambda, \boldsymbol{\alpha}) + \ln f(c/w)$. This means that in a plot of $\ln \bar{J}$ versus c/w_0 *curves of constant* λ must be *parallel* to each other—a master curve can be produced by shifting these curves vertically. Specifically, the distance between two constants λ curves is independent of geometry and is given by

$$\ln \bar{J}(\lambda_2, c/w, \boldsymbol{\alpha}) - \ln \bar{J}(\lambda_1, c/w, \boldsymbol{\alpha}) = \ln K(\lambda_2, \boldsymbol{\alpha}) - \ln K(\lambda_1, \boldsymbol{\alpha}) \tag{12}$$

As for question (iii), the above reasoning implies that $K(\lambda, \boldsymbol{\alpha}) = K(\lambda)$ if and only if the distance between curves of constant λ is *independent of material model*. These observations suggest that $\bar{J}$ should be plotted using a log scale. In the following, we plot $\ln \bar{J}$ versus c/w for different applied stretch ratios. Visual inspection of these curves will give insight on questions (ii) and (iii).

Computations using the MR model are carried out using Greensmith's material data. The elastic constants for the four rubbers used in his experiments are reported in Table 2 of Greensmith (1963). In our simulations, we select two of these rubbers (vulcanizates A and D in Table 2). These two rubbers have the largest difference in shear modulus and strain hardening behavior (reflected by C_1/C_2). Since both rubbers obey MR model, we denote them by MR1 and MR2 respectively. Specifically, the constants are

$$\text{MR1}: C_1 = 70\ \text{kPa}, C_2 = 80\ \text{kPa} (C_1/C_2 = 0.88);$$

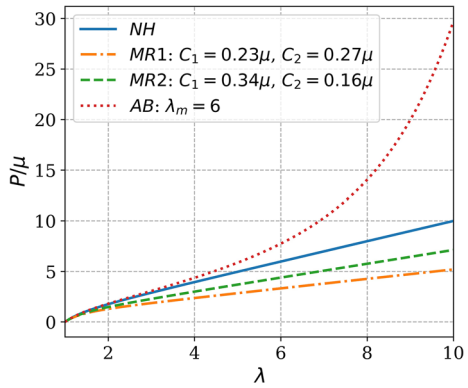

Fig. 2 Normalized nominal stress P/μ versus stretch ratio λ for NH,MR1,MR2 and AB solids

$$\text{MR2}: C_1 = 239\ \text{kPa}, C_2 = 112\ \text{kPa} (C_1/C_2 = 2.13).$$

Computations based on the AB model use $\lambda_m = 6$. Therefore, the AB solid is expected to be extremely stiff when the applied stretch ratio λ is close to 10 in simple extension. The uniaxial tension behaviors of the NH, MR1, MR2 and AB solids are shown in Fig. 2, where the nominal stress P has been normalized by the small strain shear modulus μ.

3 Finite element model (FEM)

The finite elemet model is shown schematically in Fig. 1b, and implemented in the commercial FEM software, Abaqus. Due to symmetry, only a half sample is modeled. On the bottom edge and directly ahead of the crack tip, $X_1 > c$, the vertical displacement and the shear stress are zero. On the top edge, a uniform vertical displacement Δ is imposed while the horizontal displacement is constrained to be zero. Plane stress elements CPS4 are used. The smallest element size near the crack tip is $5 \times 10^{-4} w$. Our convergence test shows that further refinement of mesh does not affect the FE results. The energy release rate can be readily extracted from Abaqus using the J-integral. The crack opening displacement and normal stress σ_{22} directly ahead of the crack tip are provided for all four material models in the ESM at a particular crack length, $c/w = 0.2$. We check our FEM results by reproducing the handbook value (see the ESM) for a wide range of c/w from 0.1 to 0.9.

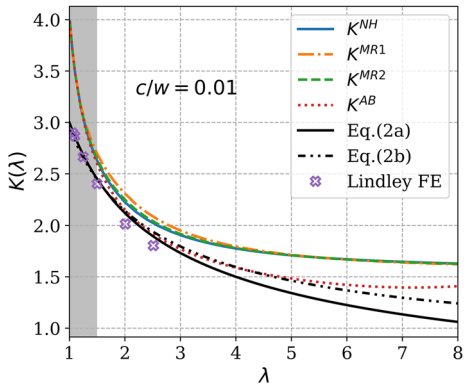

Fig. 3 The load factor $K(\lambda, \alpha)$ defined by (7) for short cracks. Since this load factor in general depends on the constitutive model, we use superscript to indicate the constitutive model, e.g. the AB in K^{AB} represents the Arruda-Boyce model

3.1 Comparison with Greensmith: short cracks

Figure 3 plots the finite element result $K(\lambda, \alpha)$ for four different solids (NH, MR1, MR2, AB). In these calculations, $c/w = 0.01$. For sufficiently small cracks, separability is expected (this will be examined in section 4.2) so $K(\lambda, \alpha)$ is computed using (6) and realizing $f(c/w << 1) = 1$. An important result is that K for the NH, MR1 and MR2 almost lie on top of each other for stretch ratios less than 8. For convenience, we call this factor $K^{MR}(\lambda)$ since there is no big differences between them. The factor for the AB model is denoted by $K^{AB}(\lambda)$. Figure 3a shows that, as expected, K is independent of the material model for small deformation. For a stretch greater than about 2 the results diverge and are increasingly different as the stretch is increased. Finally, Fig. 3 shows that $K^{AB}(\lambda)$ agrees well with $K^{MR}(\lambda)$ for $\lambda \leq 2$, after that it becomes smaller. This and the previous result of Yeoh (2002) shatters the belief that that for short crack lengths $K(\lambda, \alpha)$ is independent of material model.

Figure 3 shows discrepancy between the Greensmith's equations (2a,b) and our FE results when the strains are less than 50%. Specifically, (2a,b) underestimate $K(\lambda)$ by about 25% for $1 \leq \lambda \leq 1.5$. Note K^{MR} or K^{AB} as $\lambda \to 1$ is 4.0, slightly larger than the theoretical value of 3.95 for small cracks. Thus, our FE result approaches the theoretical limit (3) whereas the FE results of Lindley and Yeoh did not. It is interesting to note that the slope of the FE $K(\lambda)$ is much steeper than those in observed in Greensmith's experiments. This rapid decay suggests it is very difficult to determine $K(\lambda)$ experimentally in the regime of small strains and short cracks. For $1.5 \leq \lambda \leq 2.5$, there is agreement within about 10% between (2a,b) and our FE result. For larger stretch ratios, $\lambda > 2.5$, $K(\lambda)$ predicted by (2a) is significantly lower than our finite element result. Interestingly, (2b) is a *better approximation* for $\lambda > 2.5$, although it still underestimates $K(\lambda)$. It should be noted that (2a,b) are not intended to be used for $\lambda > 2$, so it is not surprising that discrepancy occurs at these larger stretches.

3.2 Normalized energy release rate for short cracks

Here we propose expressions for the energy release rate for short cracks which are accurate for a wide range of stretch ratios. As noted above, these expressions depend on the strain energy density function. For the MR solid (including neo-Hookean as a special case), J can be fit using the following simple expression:

$$J^{MR} = \left[2W_0^{MR}(\lambda)\, c\right] K^{MR}(\lambda)\, f^{MR}(c/w), \quad 1 < \lambda \leq 8 \tag{13a}$$

where

$$K^{MR}(\lambda) = \frac{1.476\lambda + 0.2111}{\lambda - 0.5804}, \quad f^{MR}(c/w << 1) = 1 \tag{13b,c}$$

Similarly, for the AB solid, we found

$$J^{AB} = \left[2W_0^{AB}(\lambda)\, c\right] K^{AB}(\lambda)\, f^{AB}(c/w), \quad 1 < \lambda \leq 8 \tag{14a}$$

$$K^{AB}(\lambda) = \frac{1.184\lambda + 0.8277}{\lambda - 0.4980}, \quad f^{AB}(c/w << 1) = 1 \tag{14b,c}$$

Explicit expressions for f^{MR} and f^{AB} will be given below.

As shown in Fig. 4, (13) and (14) compare very well with FEM results for small cracks, where $f = 1$. In the following, we shall show that, as long as $\lambda \geq 1.5$, (13) or (14) are valid, provided that $c/w \leq 0.6$. We will see that these expressions do not work well if $\lambda < 1.5$; this is because the separability assumption breaks down for small strains. In particular, the short crack approximation of Rivlin and Thomas (1953) does not work well in the small strain limit.

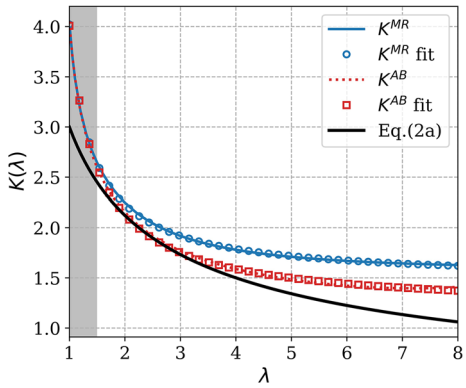

Fig. 4 Equations (13) and (14) (symbols) versus FEM results (blue solid and red dotted lines) for $c/w = 0.01$. Equation (2a) is also plotted for comparison

3.3 Energy release rate for longer cracks $c/w < 0.6$

Figure 5a plots $\ln \bar{J}$ versus c/w for different stretch ratios for MR. The special case of neo-Hookean solid ($C_2 = 0$) is provided in the ESM. *If separability exists,* then curves with different λ should be *parallel*. Figure 5a shows that *separability is not satisfied* for $1 \leq \lambda < 1.2$. There is a gradual transition as λ increases from 1.2 to 1.5, after that all the constant λ curves are parallel to each other as long as $c/w \leq 0.6$. Separability starts to break down for crack length longer than $c/w > 0.6$. However, for larger stretch ratios, e.g. $\lambda \geq 2$, separability is approximately satisfied even for $c/w = 0.9$. Since separability is *not satisfied* for $\lambda < 1.5$, (13b) should be used with great care. However, for $\lambda \geq 1.5$, separability is satisfied, meaning that (13a) *and* (13b) still work. To account for the effect of crack length in (13) $f^{MR}(c/w)$ is fit to the FEM results. We found

$$f^{MR}(c/w) = 0.9997 \exp(0.1028 c/w) + 0.0003 \exp(9.007 c/w) \quad (15)$$

We plot the approximation using (13a,b) and (15) against the FE in Fig. 5b for $1.5 \leq \lambda \leq 8$. They agree well. In the ESM, we further confirm separability by plotting $\bar{J}/K(\lambda)$ for different $\lambda \geq 1.5$ and show that the resulting curves collapse onto a single master curve, which is given by (15).

Figure 6a plots $\ln \bar{J}$ versus c/w for different stretch ratios for the AB solid. For $c/w \leq 0.6$ and $\lambda \geq 1.5$, the curves of different λ are parallel to each other indicating *separability* of load and geometry. For this case, we fit $f^{AB}(c/w)$ as

$$f^{AB}(c/w) = 0.9988 \exp(0.03329 c/w) + 0.0012 \exp(6.485 c/w) \quad (16)$$

Equations (14a,b) with (14c) replaced by (16) are plotted as dashed curves in Fig. 6b. Again, separability is approximately satisfied for larger stretch ratios, e.g. $2 \leq \lambda < 6$, even for $c/w = 0.9$. The stretch ratio that produces the large error is $\lambda \geq 6$. This is expected since the limit of extensibility in the calculation is $\lambda_m = 6$.

4 Summary and discussion

The key result in this paper is that simple expressions for the energy release rate J of a SEN specimen are developed. These expressions can be used to determine fracture toughness in tests of soft, tough materials using the SEN geometry. For the Mooney-Rivlin solid (which includes the neo-Hookean solid as a special case), J is given by (13a) with $K^{MR}(\lambda)$ given by (13b) and $f^{MR}(c/w)$ given by (15). For the AB solid, J is given by (14a) with $K^{AB}(\lambda)$ given by (14b) and $f^{AB}(c/w)$ given by (16). The solution of the AB model depends on the critical stretch λ_m which we have taken to be 6. Specifically, $K^{AB}(\lambda)$ will increase with increasing critical stretch λ_m, and approaches the NH solution at $\lambda_m = \infty$. Therefore, in general, the agreement between the AB and the MR models will improve with increasing λ_m. These expressions for J are strictly valid for $\lambda \geq 1.5$ and $c/w \leq 0.6$. However, for large stretch ratios in MR model ($\lambda \geq 2$) or in AB model ($2 \leq \lambda < 6$), these expressions still provide reasonable approximation of the energy release rate ($\sim 10\%$ error) up to $c/w = 0.9$. Our results also show that, in contrast to Greensmith's results, the energy release rate as $\lambda \to 1$ is equal to the linear elastic fracture result.

The separability of the energy release rate into a part that depends on geometry (mainly c/w) and a part that depends only on the applied stretch greatly simplifies the analysis as well as interpretation of results. An unexpected feature is that separability is favored by large stretch ratios but fails at stretch ratios below 1.5. For typical *tough* elastic solids, this is not a problem as the critical stretch ratio at failure is much larger. Our results show that the energy release rate depends on elasticity model, although this dependence is not strong, at least for the MR and AB model. Here we note that the AB model has very similar behavior to the

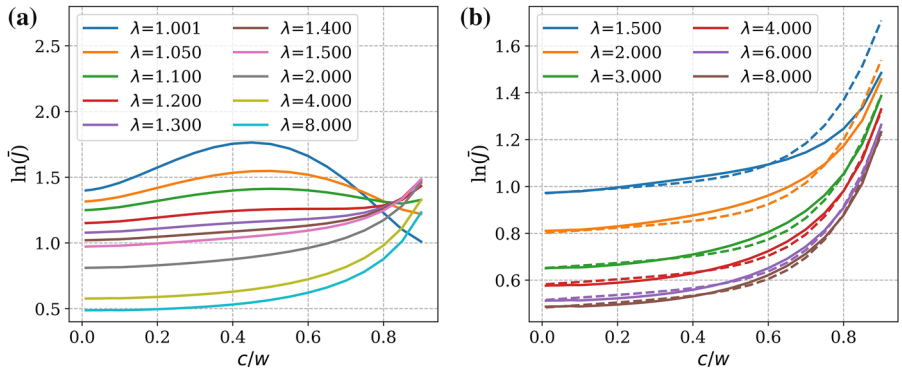

Fig. 5 **a** ln $\bar{J}$ versus c/w for the MR solid. Different curves correspond to different applied stretch ratio λ. **b** Comparison of FE results with (13a,b) with $f^{MR}(c/w)$ in (13a) replaced by (15). Solid curves are FE, dashed curves are approximate results

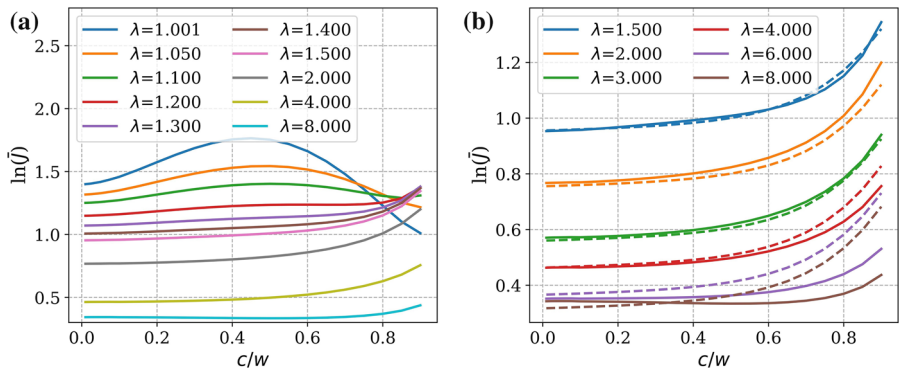

Fig. 6 **a** ln $\bar{J}$ versus c/w for the AB solid. Different curves correspond to different applied stretch ratio λ. **b** Comparison of FE results with (14a,b) with $f^{AB}(c/w)$ in (14a) replaced by (16). Solid curves are FE, dashed curves are approximate results

Gent model, so our result applies to the Gent model as well (Gent 1996; Boyce and Arruda 2000). On the other hand, Yeoh (2002) has shown considerable discrepancies between the MR and the 3-term Yeoh solid for strains in excess of 20%, so exceptions do exist. Nevertheless, this work suggests that separability is likely to hold for any material model and when in doubt, one can perform additional numerical analysis for the material of interest.

Our numerical results show that strain hardening behavior can affect the energy release rate. Indeed, the energy release rate predicted by the AB model at stretch ratios $\lambda \geq 3$ is lower than those predicted by the NH or MR model. Since strains near the crack tip are much larger than the applied stretch, significant strain hardening can occur near the crack tip. Hence, a reasonable way to determine a material model for tough materials is to conduct uniaxial tension test in uncracked sample until failure.

Acknowledgements This material is based upon work supported by the National Science Foundation under Grant No. CMMI-1903308. We are grateful to the reviewers for their helpful comments.

Funding National Science Foundation under Grant No. CMMI-1903308.

Availability of data and material This work does not have any experimental data.

Compliance with ethical standards

Conflicts of interest We declare we have no competing interests.

Code availability Abaqus input files are available in the Electronic Supplementary Material.

References

Arruda EM, Boyce MC (1993) A three-dimensional constitutive model for the large stretch behavior of rubber elastic materials. J Mech Phys Solids 41:389–412. https://doi.org/10.1016/0022-5096(93)90013-6

Bai R, Yang J, Morelle XP et al (2018) Fatigue fracture of self-recovery hydrogels. ACS Macro Lett 7:312–317. https://doi.org/10.1021/acsmacrolett.8b00045

Boyce MC, Arruda EM (2000) Constitutive models of rubber elasticity: a review. Rubber Chem Technol 73:504–523. https://doi.org/10.5254/1.3547602

Chen C, Wang Z, Suo Z (2017) Flaw sensitivity of highly stretchable materials. Extreme Mech Lett 10:50–57. https://doi.org/10.1016/j.eml.2016.10.002

Cristiano A, Marcellan A, Keestra BJ et al (2011) Fracture of model polyurethane elastomeric networks. J Polym Sci Part B 49:355–367. https://doi.org/10.1002/polb.22186

Ducrot E, Chen Y, Bulters M et al (2014) Toughening elastomers with sacrificial bonds and watching them break. Science 344:186–189. https://doi.org/10.1126/science.1248494

Gent AN (1996) A new constitutive relation for rubber. Rubber Chem Technol 69:59–61. https://doi.org/10.5254/1.3538357

Gong JP, Katsuyama Y, Kurokawa T, Osada Y (2003) Double-network hydrogels with extremely high mechanical strength. Adv Mater 15:1155–1158. https://doi.org/10.1002/adma.200304907

Greensmith HW (1963) Rupture of rubber. X. The change in stored energy on making a small cut in a test piece held in simple extension. J Appl Polymer Sci 7:993–1002. https://doi.org/10.1002/app.1963.070070316

Hamed GR, Park BH (1999) The mechanism of carbon black reinforcement of SBR and NR vulcanizates. Rubber Chem Technol 72:946–959. https://doi.org/10.5254/1.3538844

Kim JY, Liu Z, Weon BM et al (2020) Extreme cavity expansion in soft solids: damage without fracture. Sci Adv 6:eaaz0418. https://doi.org/10.1126/sciadv.aaz0418

Kundu S, Crosby AJ (2009) Cavitation and fracture behavior of polyacrylamide hydrogels. Soft Matter 5:3963. https://doi.org/10.1039/b909237d

Kwon HJ, Rogalsky AD, Kim D-W (2011) On the measurement of fracture toughness of soft biogel. Polymer Eng Sci 51:1078–1086. https://doi.org/10.1002/pen.21923

Kwon SW, Sun CT (2000) Characteristics of three-dimensional stress fields in plates with a through-the-thickness crack. Int J Fract 104:289–314. https://doi.org/10.1023/A:1007601918058

Lin W-C, Fan W, Marcellan A et al (2010) Large strain and fracture properties of poly(dimethylacrylamide)/silica hybrid hydrogels. Macromolecules 43:2554–2563. https://doi.org/10.1021/ma901937r

Lin W-C, Marcellan A, Hourdet D, Creton C (2011) Effect of polymer-particle interaction on the fracture toughness of silica filled hydrogels. Soft Matter 7:6578. https://doi.org/10.1039/c1sm05420a

Lindley PB (1972) Energy for crack growth in model rubber components. J Strain Anal 7:132–140. https://doi.org/10.1243/03093247V072132

Mayumi K, Guo J, Narita T et al (2016) Fracture of dual crosslink gels with permanent and transient crosslinks. Extreme Mech Lett 6:52–59. https://doi.org/10.1016/j.eml.2015.12.002

Morelle XP, Illeperuma WR, Tian K et al (2018) Highly stretchable and tough hydrogels below water freezing temperature. Adv Mater 30:1801541. https://doi.org/10.1002/adma.201801541

Rivlin RS, Thomas AG (1953) Rupture of rubber. I. Characteristic energy for tearing. J Polym Sci 10:291–318. https://doi.org/10.1002/pol.1953.120100303

Roucou D, Diani J, Brieu M et al (2018) Experimental investigation of elastomer mode I fracture: an attempt to estimate the critical strain energy release rate using SENT tests. Int J Fract 209:163–170. https://doi.org/10.1007/s10704-017-0251-x

Sun J-Y, Zhao X, Illeperuma WRK et al (2012) Highly stretchable and tough hydrogels. Nature 489:133–136. https://doi.org/10.1038/nature11409

Tada H, Paris PC, Irwin GR, Tada H (2000) The stress analysis of cracks handbook. ASME Press, New York

Tanaka Y, Kuwabara R, Na Y-H et al (2005) Determination of fracture energy of high strength double network hydrogels. J Phys Chem B 109:11559–11562. https://doi.org/10.1021/jp0500790

Wigglesworth LA (1957) Stress distribution in a notched plate. Mathematika 4:76–96. https://doi.org/10.1112/S002557930000111X

Yeoh OH (2002) Relation between crack surface displacements and strain energy release rate in thin rubber sheets. Mech Mater 34:459–474. https://doi.org/10.1016/S0167-6636(02)00174-6